Supporting Information

Manganese cluster-based MOF as efficient polysulfide-trapping platform for high-performance lithium-sulfur batteries

Xiao-Fei Liu,[a] Xiao-Qing Guo, [a] Rui Wang, [a] Qing-Chao Liu,* [a] Zhong-Jun Li, [a] Shuang-Quan Zang,* [a] and Thomas C. W. Mak [a, b]

[a] College of Chemistry and Molecular Engineering, Zhengzhou University, Zhengzhou 450001, China

[b] Department of Chemistry and Center of Novel Functional Molecules, The Chinese University of Hong Kong, Shatin, New Territories Hong Kong SAR, China

Author for correspondence: **Prof. S.-Q. Zang; Dr. Q.-C. Liu**

EXPERIMENTAL SECTION

Materials.

Except where mentioned, all of the materials for synthesizing were obtained commercially and used without further purification. All the solvents used in experiments were of analytical grade.

Instrumentation and Measurements

^{1}H and ^{13}C NMR spectra were recorded on a Bruker DRX spectrometer operating at 400 MHz in DMSO-d_6. Elemental analyses (EA) were gained using a Perkin-Elmer 240 elemental analyzer. Powder X-ray diffraction (PXRD) patterns of the samples were implemented on a Rigaku B/Max-RB diffractometer. Thermogravimetry analyses (TGA) were performed on a TA Q50 system under N_2 atmosphere at a heating rate of 10 ^{o}C min^{-1}. Water sorption isotherms at 298 K were measured by a BEL-max physisorption analyzer after soaked the samples in methanol for 3 days with renewal once a day and then pretreated under vacuum at 150 ^{o}C for 12 h. X-ray photoelectron spectroscopy (XPS) measurements were performed with a VG Scientific ESCALAB 250 instrument. The morphology and microstructure of the fabricated materials are characterized by a field emission scanning electron microscopy, JEOL model JSM-6700 FE-SEM, operating at an accelerating voltage of 1.5 or 5.0 kV. The CV of coin cells was measured with a two-probe method with CHI660e electrochemical working station (CH Instrument Inc.). Electrical measurements were performed in air at a constant temperature of 298 K. The Nyquist plots of the samples were studied by CompactStat-Plus2 (Ivium) in a frequency range of 0.1Hz to 100000 Hz.

Single-Crystal X-ray Diffraction Analyses

Single-crystal X-ray diffraction (SCXRD) measurements of **Mn-CCs-xH_2O** and **Mn-CCs** were performed on a Rigaku XtaLAB Pro diffractometer with Cu-Kα radiation (λ = 1.54178 Å) at variable temperatures. All structures were solved by the direct method [1] and refined with the full-matrix least-squares technique on F^2 by the *SHELXTL*-2013 software package.[2] All the non-hydrogen atoms were refined anisotropically. Fourier difference maps (F_o-F_c) in bitmap and contour styles were both computed in the WinGX program system. Other hydrogen atoms were placed geometrically. Displacement parameter restraints were used in modeling the ligands and solvent molecules. Hydrogen atoms were placed geometrically on their riding atom where possible. The diffuse electron densities resulting from the residual solvent molecules were removed from the data set using the SQUEEZE routine of PLATON and further refined using the data generated.[3] The contents of the solvent region are not represented in the unit cell contents in the crystal data. Detailed structure determination parameters and crystallographic data are given in Table S1. Relevant bond lengths and bond angles are displayed in Table S2. More details on the crystallographic data are given in the X-ray crystallographic files in CIF format. As for the pre-experiments of single crystal X-ray diffraction during the transformation from **Mn-CCs-xH_2O** to **Mn-CCs**, the crystal was fixed on goniometer head and test in situ after being automatically immersed in N_2 atmosphere for a certain period of time. Crystallographic data for the structure reported in this paper have also been deposited with CCDC (No. 1865016-1865015).

Synthesis of the H_4L ligand

H_4L was synthesized according to the reference.[4]

Synthesis of Mn-CCs-xH_2O ($[Mn_{1.125}(OH)_{0.25}(H_2O)_{1.75}L_{0.5}]_n$)

The ligand 5-phosphonomethyl-isophthalic acid (H_4L) was synthesized according to the reference (**Scheme S1**) and characterized by ^{1}H NMR and ^{13}C NMR (Supporting information). In the typical procedure, a solution of $MnCl_2 \cdot 4H_2O$ (197.8 mg, 1 mmol) and H_4L (260.1 mg, 1 mmol) in 40 mL N, N-dimethyl

formamide and deionized water (v/v, 1/1) was added in a 100 mL teflon-lined stainless steel container and heated at 140 ^{o}C for 3 days and then cooled to room temperature. Colorless cubical block crystals of **Mn-CCs-xH_2O** were collected and washed with deionized water. Yield: 75% based on manganese. Elemental analysis, Calcd (%) for $C_{36}H_{50}Mn_9O_{44}P_4$ (1805.10): C 23.95, H 2.79, P 6.86; Found (%): C 24.01, H 2.78, P 6.91. And the nanoparticle of **Mn-CCs-xH_2O** was synthesized with the addition of 1 mL ammonium hydroxide in above mixed solution and used for property tests.

Synthesis of Mn-CCs ($[Mn_{1.125}(OH)_{0.25}L_{0.5}]_n$)

The H_2O adsorption isotherm of **Mn-CCs-xH_2O** (**Figure 3b**) proved that it can absorb H_2O at very low relative humidity (RH). To remove the guest solvent in **Mn-CCs-xH_2O**, the powder of **Mn-CCs-xH_2O** was soaked in methanol for 3 days and then filtered and dried in surrounding condition and further heated at 150 ℃ under vacuum conditions for 12 h to obtain the activated **Mn-CCs**.

Preparation of S@Mn-CCs

The activated **Mn-CCs** and sulfur with the mass ratio of 3:7 were mixed by hand-milling in an Ar filled glovebox (O_2, H_2O < 0.1 ppm) and fabricated through melt-diffusion method at 155 ℃ in a teflon-lined stainless steel container filled with Ar for 12 h. After cooling to room temperature, S@**Mn-CCs** cathode materials were collected.

Preparation of S@CNTs

The synthesis procedure is similar to that of S@Mn-CCs.

Preparation of S/Mn-CCs

The activated **Mn-CCs** and sulfur with the mass ratio of 3:7 were mixed by hand-milling in an Ar filled glovebox (O_2, H_2O < 0.1 ppm).

Fabrication of the coin Li-S battery

70 wt% S@**Mn-CCs** composite, 20 wt% CNTs and 10 wt% poly(vinylidene fluoride) (PVDF) binder were mixed in N-methyl-2-pyrrolidinone (NMP) to form a slurry. The slurry was then coated on carbolic current collectors as cathode and dried at 60 ℃ for 12 h. Coin cells 2025 were assembled in an Ar filled glovebox (O_2, H_2O < 0.1 ppm) with an electrolyte of 1.0 M lithium ditrifluoromethanesulfonate (LiTFSI) and 0.1 M $LiNO_3$ in DOL/DME (v/v, 1/1), Celgard 2400 membrane, and Li foil reference anode. For all of the electrochemical tests, the sulfur mass loading was about 2.0 mg/cm^2.

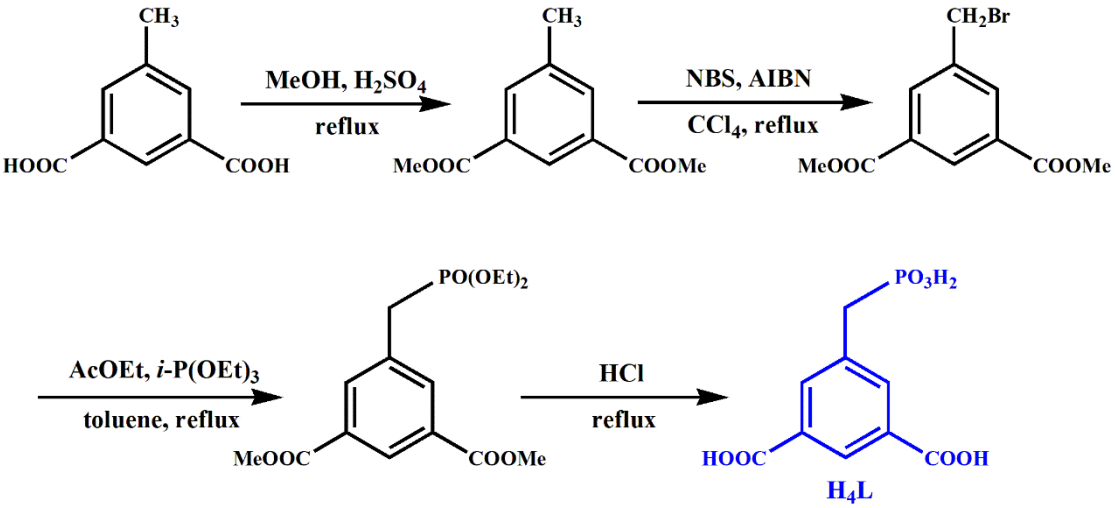

Scheme S1. Synthesis of the ligand H_4L.

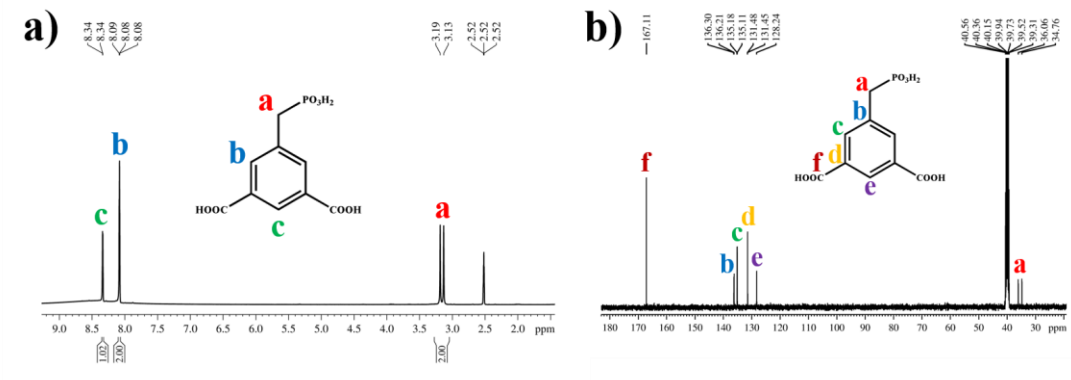

Fig. S1 ^{1}H (a) and ^{13}C (b) NMR of H_4L ligand.

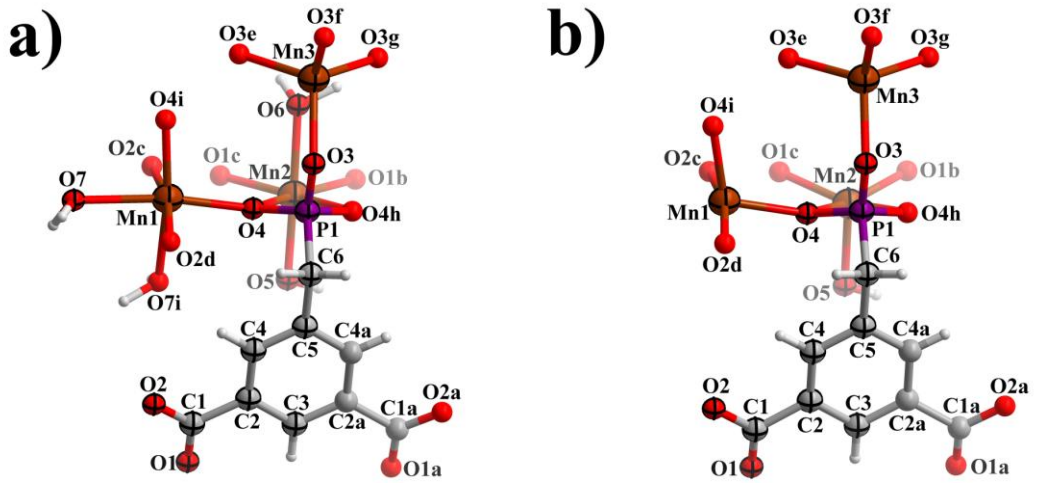

Fig. S2 Perspective views of the coordination environments in (a) **Mn-CCs-xH$_2$O** and (b) **Mn-CCs**. Symmetry codes: (a) a = *x*, *y*, 1-*z*; b = *y*, *z*, 1-*x*; c = *y*, *z*, *x*; d = 1/2-*x*, 1/2-*z*, 1/2-*y*; e = -1/2+*z*, 1/2-*y*, 1/2-*x*; f = -*x*, *y*, 1-*z*; g = 1/2-*z*, 1/2-*y*, 1/2+*x*; h = *x*, *y*, 1-*z*; i = 1/2-*z*, 1/2-*y*, 1/2-*x*; (b) a = 1-*x*, *y*, *z*; b = *z*, 1-*x*, y; c = 1-*z*, 1-*x*, *y*; d = 1/2+*y*, -1/2+*x*, 1/2-*z*; e = 1/2+*z*, 1/2-*y*, -1/2+*x*; f = *x*, *y*, -*z*; g = 1/2-*z*, 1/2-*y*, -1/2+*x*; h = 1-*x*, *y*, *z*; i = 1/2+*z*, 1/2-*y*, -1/2+*x*.

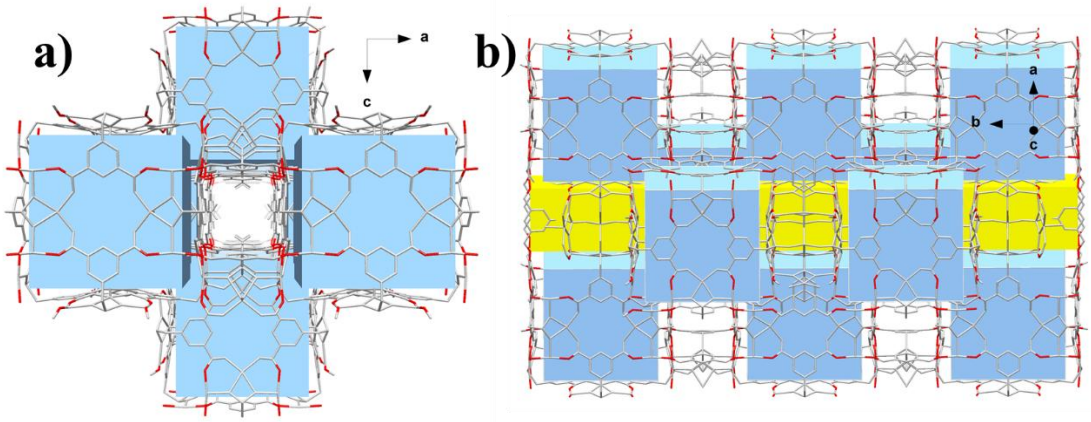

Fig. S3 Perspective views of 1D channel stacked by cages in **Mn-CCs-xH$_2$O** along (a) *b* axis and (b) *c* axis.

Table S1 Crystal structure and refinement details of MOFs

	Mn-CCs-xH_2O	Mn-CCs
Empirical formula	$C_{36}H_{50}Mn_9O_{44}P_4$	$C_{36}H_{22}Mn_9O_{30}P_4$
Formula weight	1805.10	1552.87
Temperature / K	100	500
Crystal system	cubic	cubic
Space group	$Pm\bar{3}n$	$Pm\bar{3}n$
a/Å	22.5987(2)	22.2297(2)
b/Å	22.5987(2)	22.2297(2)
c/Å	22.5987(2)	22.2297(2)
α/°	90	90
β/ °	90	90
γ/ °	90	90
Volume/$Å^3$	11541.2(3)	10985.0(3)
Z	6	6
Density (calculated) / g cm^{-3}	1.557	1.378
Absorption coefficient / mm^{-1}	13.182	13.583
F(000)	5418.0	4470.0
Reflections collected	25236	10898
Independent reflections	2285	1798
Data / restraints / parameters	1786/24/134	1798/12/100
Goodness-of-fit on F^2	1.071	1.077
$^aR_1$, $^bwR_2$ [$I > 2\sigma(I)$]	0.0595, 0.1722	0.1158, 0.3645
$^aR_1$, $^bwR_2$ (all data)	0.0614, 0.1752	0.1349, 0.3822

$R_1 = \Sigma||F_o| - |F_c||/\Sigma|F_o|$. $wR_2 = [\Sigma w(F_o^2 - F_c^2)^2/\Sigma w(F_o^2)^2]^{1/2}$.

Table S2 Selected bond distances (Å) and angles (°) for **Mn-CCs-xH_2O** and **Mn-CCs**.

Mn-CCs-xH_2O			
Mn1−O2c	2.111(3)	Mn2−O4	2.272(3)
Mn1−O4	2.133(4)	Mn2−O5	2.130(11)
Mn1−O7	2.288(5)	Mn2−O6	2.219(6)
Mn2−O1c	2.110(4)	Mn3−O3	2.116(5)
O2c−Mn1−O2d	168.4(3)	O1b−Mn2−O6	84.9(2)
O2c−Mn1−O4	93.94(14)	O1c−Mn2−O4	95.55(13)
O2c−Mn1−O4i	93.38(14)	O1c−Mn2−O4h	159.78(14)
O2c−Mn1−O7	88.22(18)	O1c−Mn2−O5	92.1(3)
O2c−Mn1−O7i	83.02(19)	O1c−Mn2−O6	84.9(2)
O2d−Mn1−O4	93.38(14)	O4−Mn2−O4h	64.85(15)
O2d−Mn1−O4i	93.94(14)	O4−Mn2−O5	94.1(3)
O2d−Mn1−O7	83.02(19)	O4−Mn2−O6	89.97(19)
O2d−Mn1−O7i	88.22(18)	O4h−Mn2−O5	94.1(3)
O4−Mn1−O4i	101.79(18)	O4h−Mn2−O6	89.97(19)
O4−Mn1−O7	169.72(18)	O5−Mn2−O6	175.1(4)
O4−Mn1−O7i	88.09(17)	O3−Mn3−O3e	111.17(13)
O4i−Mn1−O7	88.09(17)	O3−Mn3−O3f	106.1(3)
O4i−Mn1−O7i	169.72(18)	O3−Mn3−O3g	111.17(13)
O1b−Mn2−O1c	103.4(2)	O3e−Mn3−O3f	111.17(13)
O1b−Mn2−O4	159.77(14)	O3e−Mn3−O3g	106.1(3)
O1b−Mn2−O4h	95.55(13)	O3f−Mn3−O3g	111.17(13)
O1b−Mn2−O5	92.1(3)		
Mn-CCs			
Mn1−O2c	2.044(8)	Mn2−O4	2.225(6)
Mn1−O4	2.079(6)	Mn2−O5	1.81(5)
Mn2−O1c	2.021(9)	Mn3−O3	2.053(10)
O2c−Mn1−O2d	166.3(6)	O1c−Mn2−O4h	151.2(4)
O2c−Mn1−O4	95.8(3)	O1c−Mn2−O5	97.9(13)
O2c−Mn1−O4i	92.0(3)	O4−Mn2−O4h	64.7(3)
O2d−Mn1−O4	95.8(3)	O4−Mn2−O5	105.7(16)
O2d−Mn1−O4i	92.0(3)	O4h−Mn2−O5	105.7(16)
O4−Mn1−O4i	109.8(4)	O3−Mn3−O3e	108.5(3)
O1b−Mn2−O1c	99.5(6)	O3−Mn3−O3f	111.4(6)
O1b−Mn2−O4	151.2(4)	O3−Mn3−O3g	108.5(3)
O1b−Mn2−O4h	93.4(3)	O3e−Mn3−O3f	108.5(3)
O1b−Mn2−O5	97.9(13)	O3e−Mn3−O3g	111.4(6)
O1c−Mn2−O4	93.4(3)	O3f−Mn3−O3g	108.5(3)

Symmetry codes: (a) b = *y*, *z*, 1-*x*; c = *y*, *z*, *x*; d = 1/2-*x*, 1/2-*z*, 1/2-*y*; e = -1/2+*z*, 1/2-*y*, 1/2-*x*; f = -*x*, *y*, 1-*z*; g = 1/2-*z*, 1/2-*y*, 1/2+*x*; h = *x*, *y*, 1-*z*; i = 1/2-*z*, 1/2-*y*, 1/2-*x*; (b) 1-*x*, y; c = 1-*z*, 1-*x*, *y*; d = 1/2+*y*, -1/2+*x*, 1/2-*z*; e = 1/2+*z*, 1/2-*y*, -1/2+*x*; f = *x*, *y*, -*z*; g = 1/2-*z*, 1/2-*y*, -1/2+*x*; h = 1-*x*, *y*, *z*; i = 1/2+*z*, 1/2-*y*, -1/2+*x*.

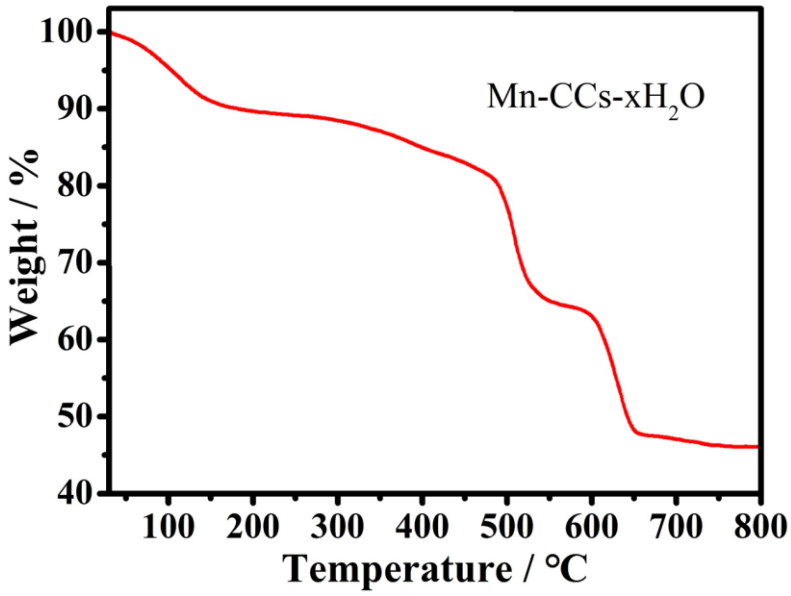

Fig. S4 TGA of sample **Mn-CCs-xH_2O**.

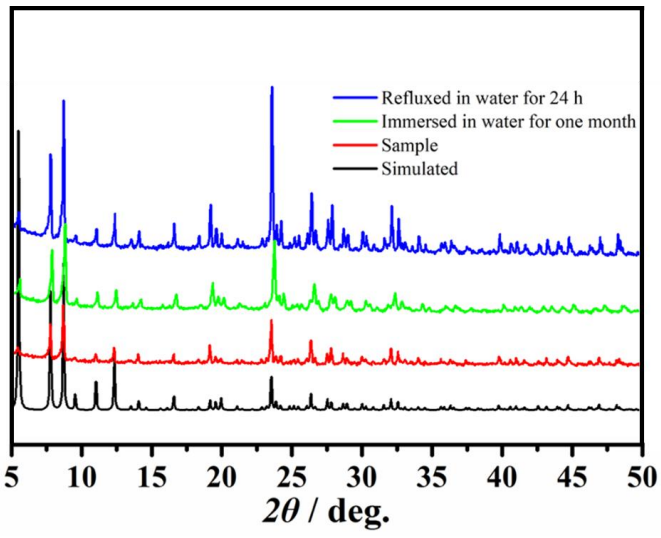

Fig. S5 PXRD patterns of **Mn-CCs-xH_2O** samples soaked in water for one month and in boiling water for 24 hours.

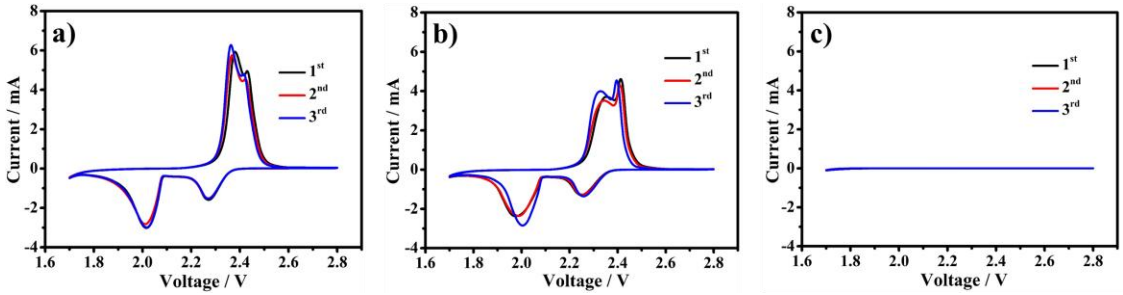

Fig. S6 CV curves of (a) S@**Mn-CCs**, (b) S@CNTs and (c) **Mn-CCs** cathodes for the first three cycles at a scan rate at 0.1 mV s^{-1} in the voltage range of 1.7-2.8 V.

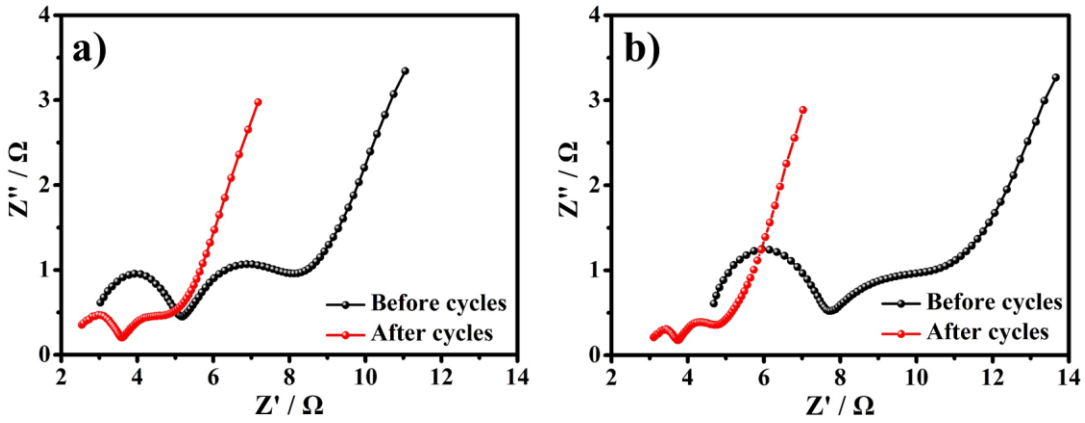

Fig. S7 Nyquist plots of batteries with (a) S@**Mn-CCs** and (b) S@CNTs before and after 10 cycles.

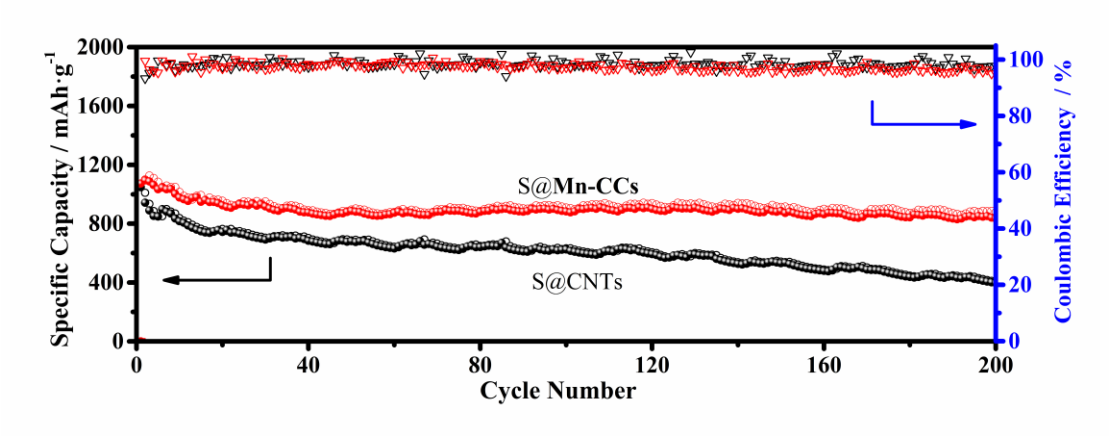

Fig. S8 Cycling stability of the S@**Mn-CCs** and S@CNTs cathodes at 0.5 C.

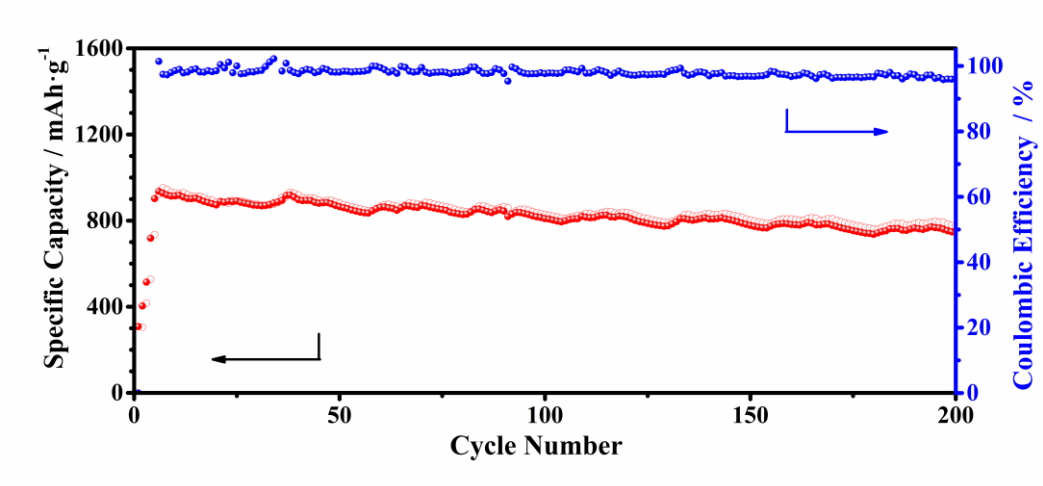

Fig. S9 Cycling stability of the S@**Mn-CCs** cathodes at 1.0 C.

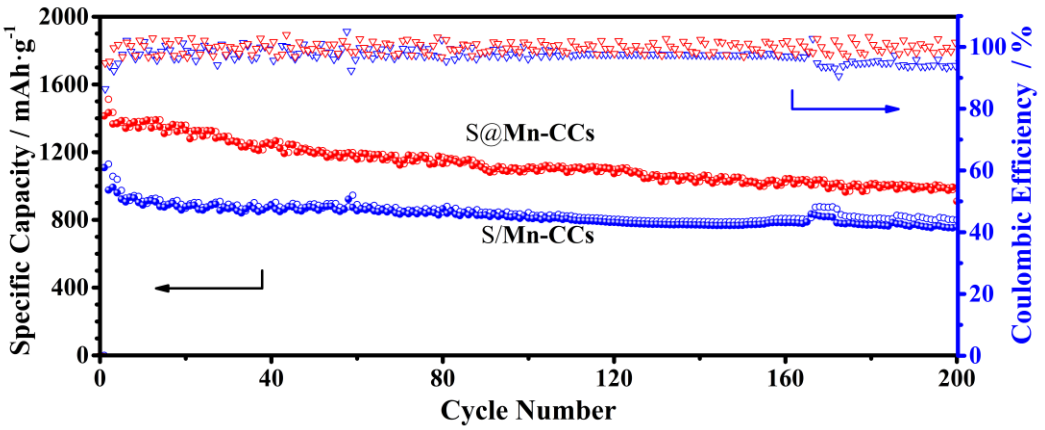

Fig. S10 Cycling stability of the S@**Mn-CCs** and S/**Mn-CCs** cathodes at 0.2 C.

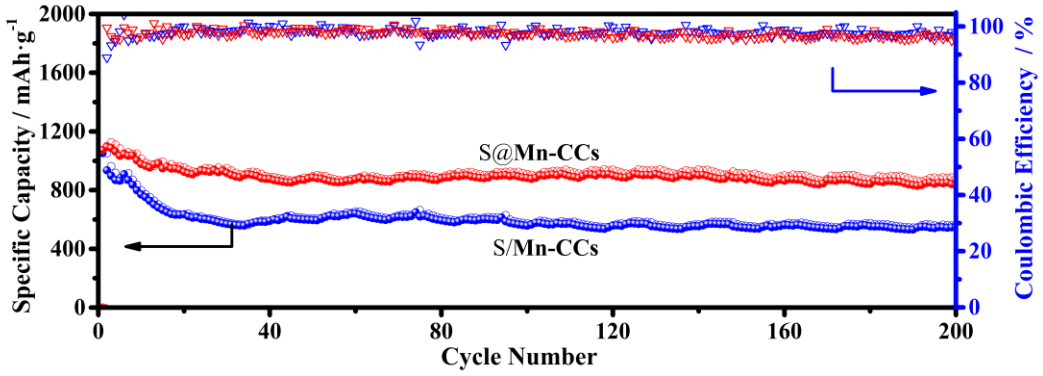

Fig. S11 Cycling stability of the S@**Mn-CCs** and S/**Mn-CCs** cathodes at 0.5 C.

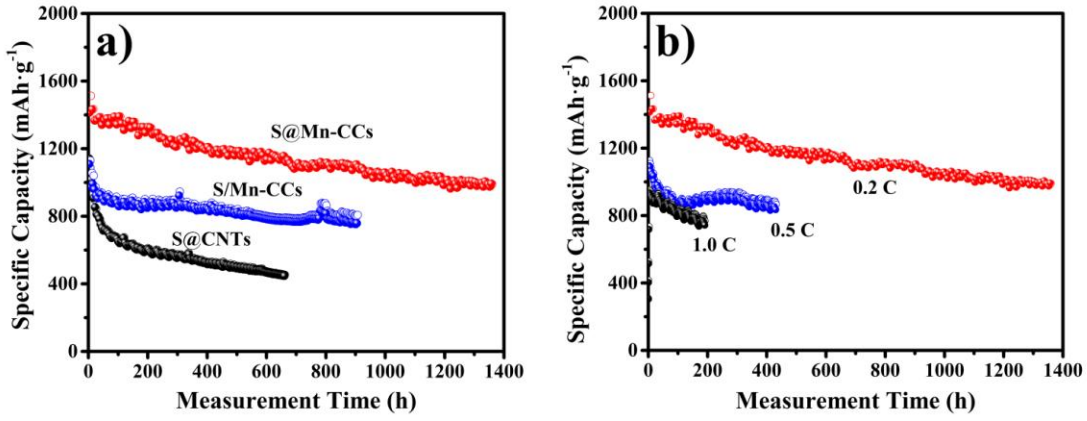

Fig. S12 Cycling stability within 200 cycles for (a) samples at 0.2 C and (b) S@**Mn-CCs** at different cycling rates.

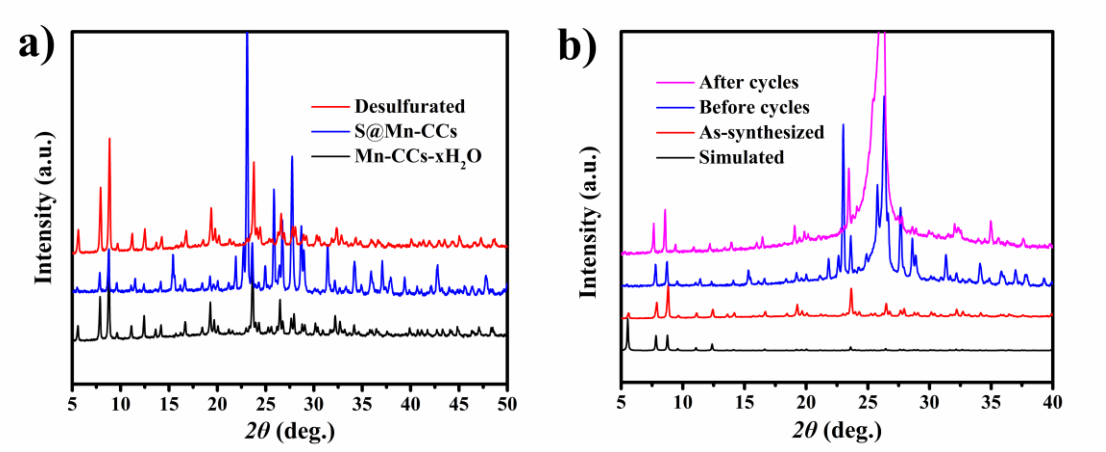

Fig. S13 PXRD spectra of (a) desulfurated S@**Mn-CCs** and (b) the cathode discharged thoroughly after 100 cycles. The cathode was washed with CS_2, acetonitrile and ethanol successively.

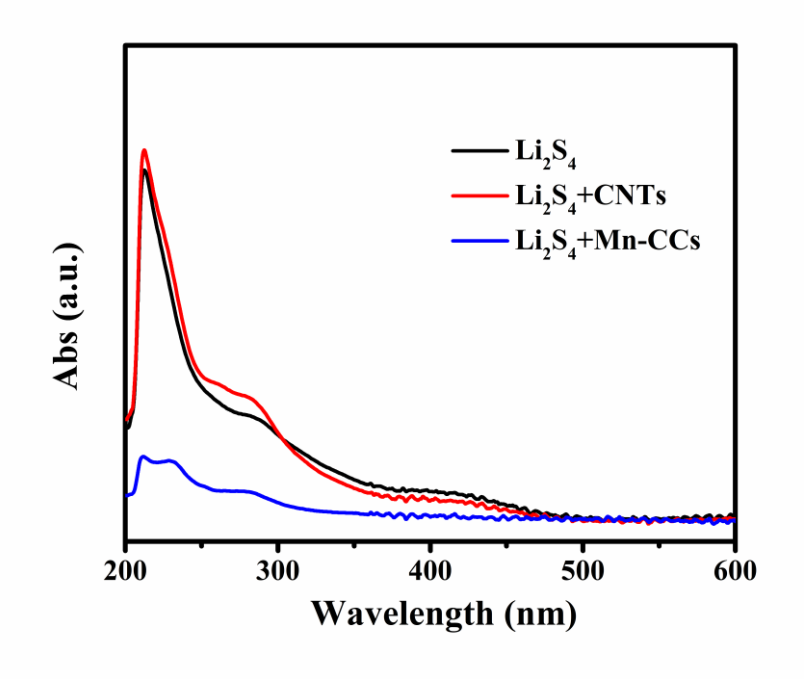

Fig. S14 UV-Vis spectra of Li_2S_4 solution before and after the addition of samples.

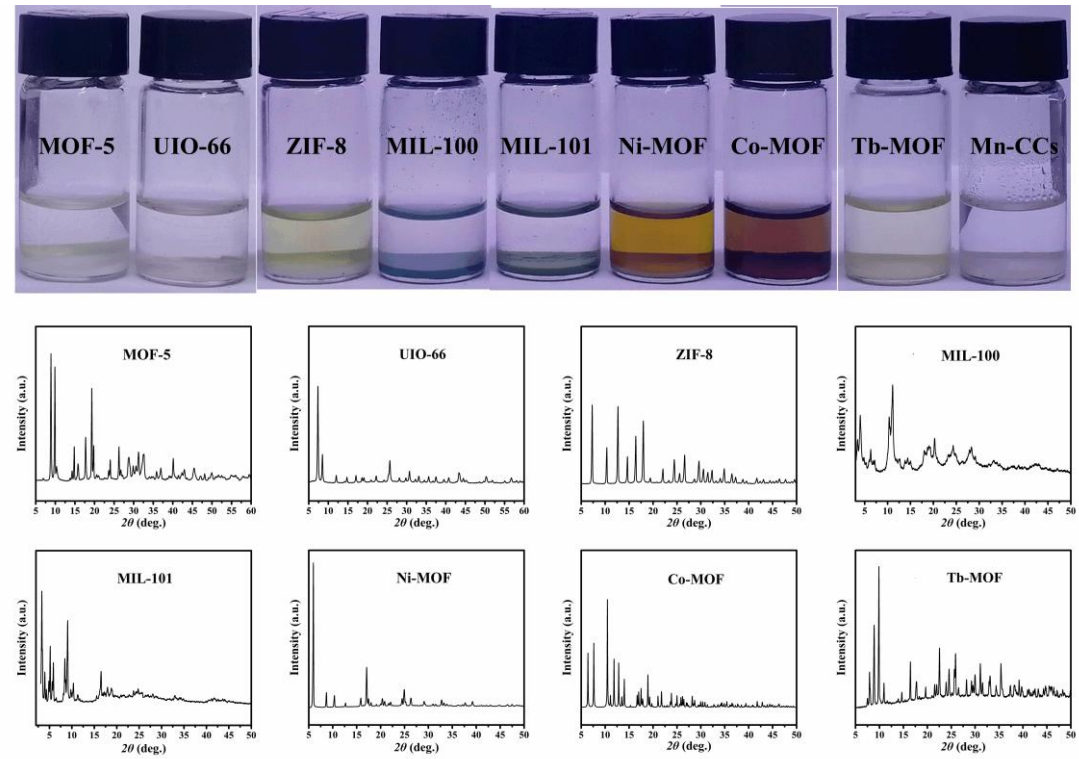

Fig. S15 Adsorption behavior of Li_2S_4 by different MOFs. (MOF-5: ref. S5; UIO-66: ref. S6; ZIF-8: ref. 27; MIL-100: ref. S15; MIL-101: ref. 28; Ni-MOF: ref. S7; Co-MOF: ref. S8; Tb-MOF: ref. S9)

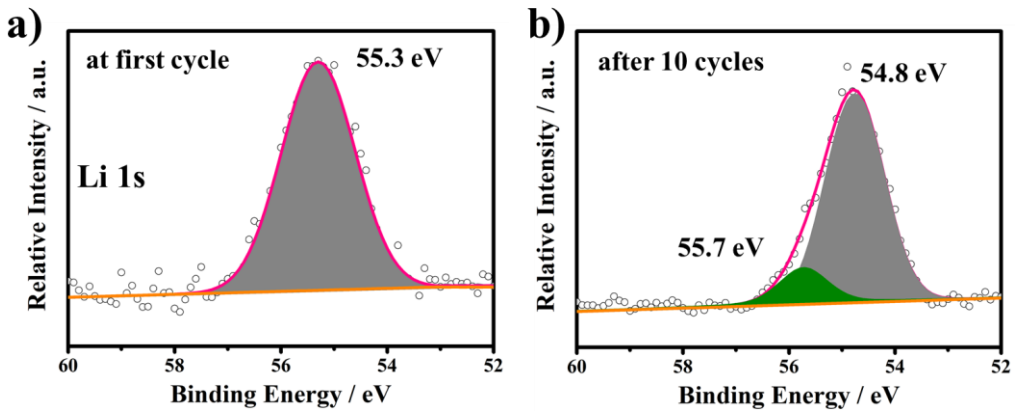

Fig. S16 Li 1s XPS spectra of the cathode S@**Mn-CCs** discharged to 2.0 V (a) at first cycle and (b) after 10 cycles.

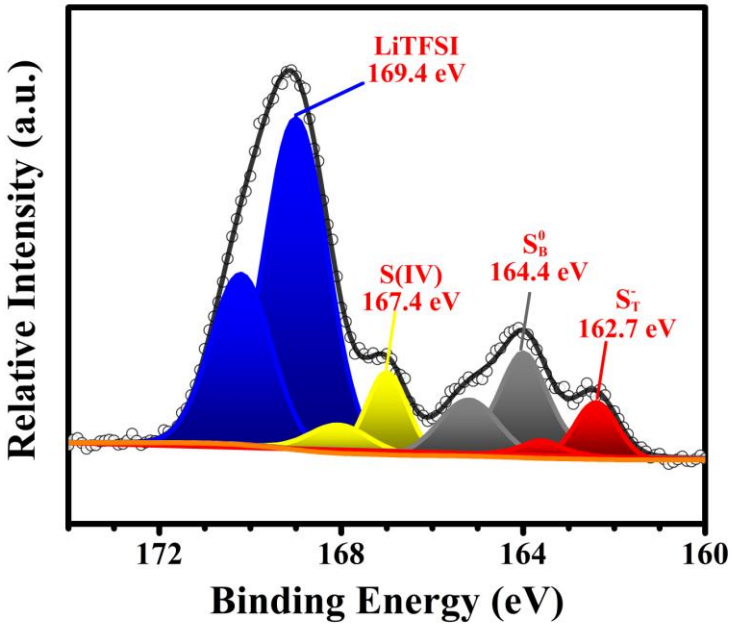

Fig. S17 XPS of S 2p spectra of a pristine battery with the cathode of S@CNTs recharged after 10 cycles.

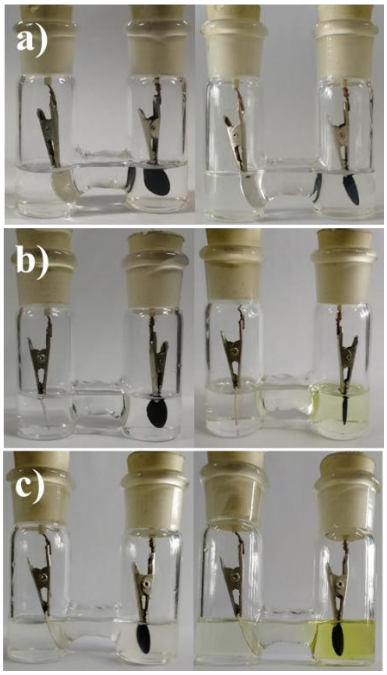

Fig. S18 Visual confirmation of LiPSs entrapment under discharge condition (100 mA g^{-1}): (a) S@**Mn-CCs**, (b) S/**Mn-CCs** and (c) S@CNTs, respectively.

Table S3 A summary of MOFs as the cathode of Li-S battery [7]

MOF used	Feature	S loading wt%	Specific capacity mAh g^{-1}	Current density C	Cycle number	Voltage vs. Li/Li^+ V	Reference	Metal
ZIF-8	Cage-like pores	50	553	0.5	300	1.8-2.8	27	Zn
HKUST-1	Lewis acidic Cu(II) site	50	286	0.5	300	1.8-2.8	27	Cu
NH_2-MIL-53	NH_2 group	50	332	0.5	300	1.8-2.8	27	Al
MIL-53	1D channel	50	347	0.5	300	1.8-2.8	27	Al
MIL-101(Cr)	Cage-like pores	48	410	0.1	60	1.0-3.0	28	Cr
MIL-101(Cr)	Graphene wrapping	58.8	809	0.8	134	1.0-3.0	29	Cr
HKUST-1	CNT interpenetration	1 mg cm^{-2}	700	0.2	500	1.7-2.8	30	Cu
MOF-5	CNT interpenetration	1 mg cm^{-2}	770	0.2	50	1.7-2.8	30	Zn
ZIF-8	CNT interpenetration	1 mg cm^{-2}	600	0.2	50	1.7-2.8	30	Zn
MOF-525	Lewis acidic Cu(II) site	50	700	0.5	200	1.5-3.0	31	Cu
$Ni_6(BTB)_4(BP)_3$	Lewis acidic Cu(II) site	60	611	0.1	100	1.5-3.0	38	Ni
ZIF-8	Cage-like pores	30	510	0.1	100	1.0-3.0	S10	Zn
MIL-101(Cr)	rGO substrate	50	650	0.2	50	1.5-3.0	S11	Cr
nMOF-867	Nitrogen atoms in linkers	50	790	0.5	100	1.7-2.8	S12	Zr
ZIF-8	200 nm particle siz	54	60	0.5	250	1.8-2.8	S13	Zn
Cd-based MOF	Semiopen channel	72	799	0.1	50	1.5-3.0	S14	Cd
MIL-100(V)	rGO substrate	50	650	0.1	75	1.6-3.0	S15	V
ZIF-8	800 nm	24	170	0.2	1000	1.4-3.0	S16	Zn
ZIF-67	1 μm	21	150	0.2	1000	1.4-3.0	S16	Co
HKUST-1	500 nm	32	250	0.2	1000	1.4-3.0	S16	Cu
Mn-CCs	Cubic cages & Lewis acidic Mn(II) site	70	990 743	0.2 1.0	200 200	1.7-2.8	This work	Mn

References

S1 G. M. Sheldrick, *SHELXS-97, Program for Solution of Crystal Structures*, University of Göttingen, Germany, 1997.

S2 G. M. Sheldrick, *SHELXL-97, Program for Crystal Structures Refinement*, University of Göttingen, Germany, 1997.

S3 A. L. Spek, *J. Appl. Crystallogr.* 2003, **36**, 7−13.

S4 Y.-S. Wei, X.-P. Hu, Z. Han, X.-Y. Dong, S.-Q. Zang and T. C. W. Mak, *J. Am. Chem. Soc.* 2017, **139**, 3505−3512.

S5 Y. Zhang, J. Zhou, X. Chen, Q. Feng and W. Cai, *J. Alloy. Compd.*, 2019, **777**, 109−118.

S6 J. H. Cavka, S. Jakobsen, U. Olsbye, N. Guillou, C. Lamberti, S. Bordiga and K. P. Lillerud, *J. Am. Chem. Soc.*, 2008, **130**, 13850–13851.

S7 R. A. Agarwal, A. Aijaz, C. Sañudo, Q. Xu and P. K. Bharadwaj, *Cryst. Growth Des.*, 2013, **13**, 1238−1245.

S8 X.-Y. Dong, B. Li, B.-B. Ma, S.-J. Li, M.-M. Dong, Y.-Y. Zhu, S.-Q. Zang, Y. Song, H.-W. Hou and T. C. W. Mak, *J. Am. Chem. Soc.*, 2013, **135**, 10214−10217

S9 X.-Y. Dong, R. Wang, J.-Z. Wang, S.-Q. Zang and T. C. W. Mak, *J. Mater. Chem. A*, 2015, **3**, 641–647.

S10 Z. Wang, Z. Dou, Y. Cui, Y. Yang, A. Wang and G. Qian, *Microporous Mesoporous Mater.*, 2014, **185**, 92−96.

S11 W. Bao, Z. Zhang, Y. Qu, C. Zhou, X. Wang and J. Li, *J. Alloys Compd.*, 2014, **582**, 334−340.

S12 J. H. Park, K. M. Choi, D. K. Lee, B. C. Moon, S. R. Shin, M.-K. Song and J. K. Kang, *Sci. Rep.*, 2016, **6**, 25555.

S13 J. Zhou, X. Yu, X. Fan, X. Wang, X. Wang, H. Li, Y. Zhang, W. Li, J. Zheng, B. Wang and X. Li, *J. Mater. Chem. A*, 2015, **3**, 8272−8275.

S14 M. T. Li, Y. Sun, K. S. Zhao, Z. Wang, X.-L. Wang, Z.-M. Su and H.-M. Xie, *ACS Appl. Mater. Interfaces*, 2016, **8**, 33183−33188.

S15 Y. Hou, H. Mao and L. Xu, *Nano Res.*, 2016, **10**, 344-353.

S16 L. Bai, D. Chao, P. Xing, L. J. Tou, Z. Chen, A. Jana, Z. X. Shen and Y. Zhao, *ACS Appl. Mater. Interfaces*, 2016, **8**, 14328−14333.